

# Biopolymer Production in a Full-Scale Activated Sludge Wastewater Treatment Plant: Seasonal Changes and Promising Bacterial Producers

Agnieszka Cydzik-Kwiatkowska <sup>1,\*</sup>, Sławomir Ciesielski <sup>1</sup>, Maciej Florczyk <sup>1</sup>, Sylwia Pasieczna-Patkowska <sup>2</sup>, Małgorzata Komorowska-Kaufman <sup>3</sup>, Weronika Pomian <sup>4</sup>, Kinga Józwiak <sup>4</sup> and Piotr Oleskowicz-Popiel <sup>3</sup>

<sup>1</sup> Faculty of Geoengineering, University of Warmia and Mazury in Olsztyn, Słoneczna 45G, 10-709 Olsztyn, Poland; slavcm@uwm.edu.pl (S.C.); maciej.florczyk@uwm.edu.pl (M.F.)

<sup>2</sup> Faculty of Chemistry, Maria Curie-Skłodowska University, pl. Marii Curie-Skłodowskiej 3/425, 20-400 Lublin, Poland; sylwia.pasieczna-patkowska@mail.umcs.pl

<sup>3</sup> Faculty of Environmental Engineering and Energy, Poznan University of Technology, Berdychowo 4, 60-965 Poznan, Poland; malgorzata.komorowska-kaufman@put.poznan.pl (M.K.-K.); piotr.oleskowicz-popiel@put.poznan.pl (P.O.-P.)

<sup>4</sup> AQUANET S.A., Dolna Wilda 126, 61-492 Poznan, Poland; weronika.pomian@aquanet.pl (W.P.); kinga.jozwiak@aquanet.pl (K.J.)

\* Correspondence: agnieszka.cydzik@uwm.edu.pl; Tel.: +48895234194

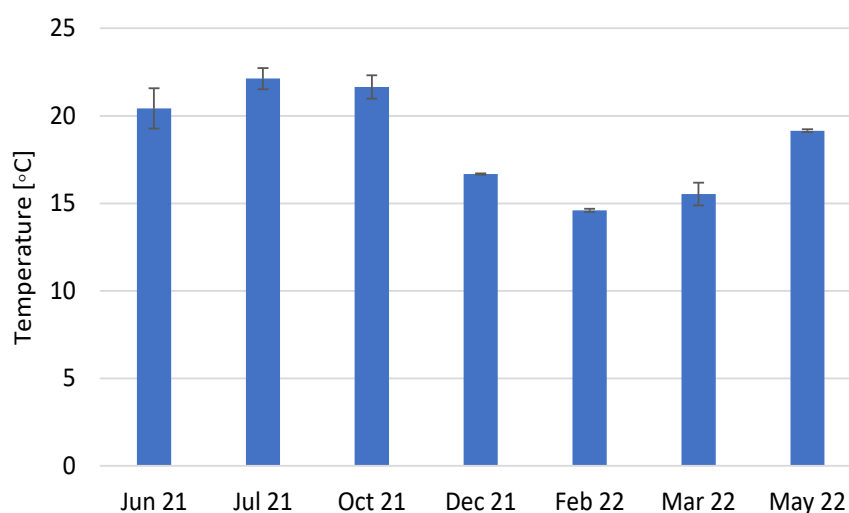


**Figure S1.** Changes in temperature in biological reactors during the study period (average of 3 reactors, n = 6000).

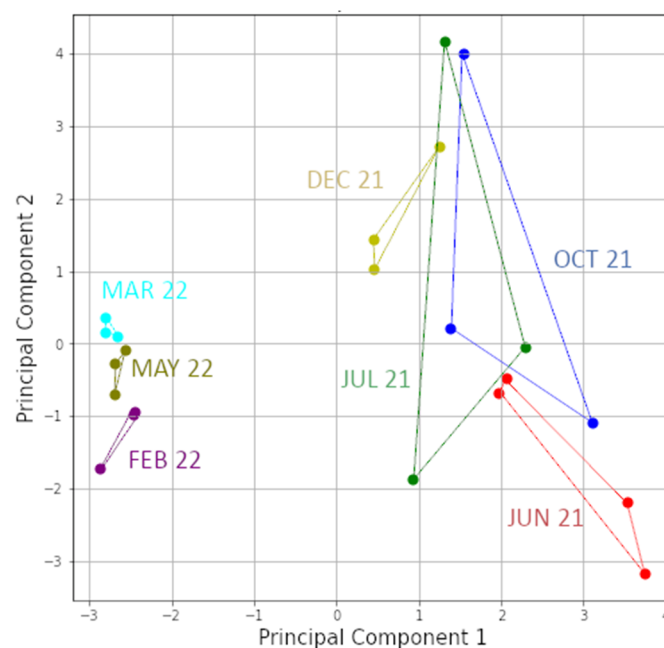


**Figure S2.** Principal component analysis based on the content of PN, PS, TOC, DOC, and POC in three EPS fractions (SOL, LB, TB) and temperature.

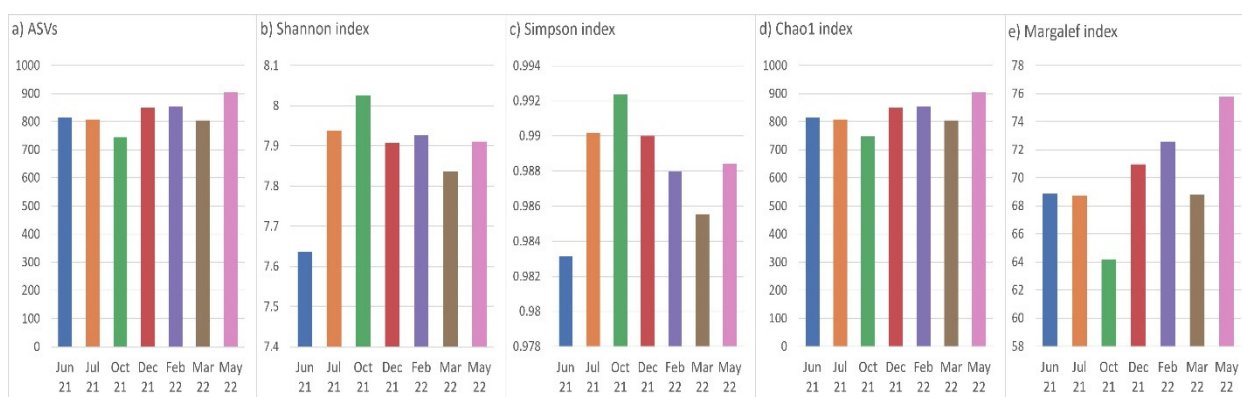


**Figure S3.** Alpha diversity metrics: a) total ASVs, b) Shannon index, c) Simpson index, d) Chao1 index, e) Margalef index of activated sludge samples obtained during the year. The color of each bar corresponds to the color used in Fig. 5 of the manuscript.

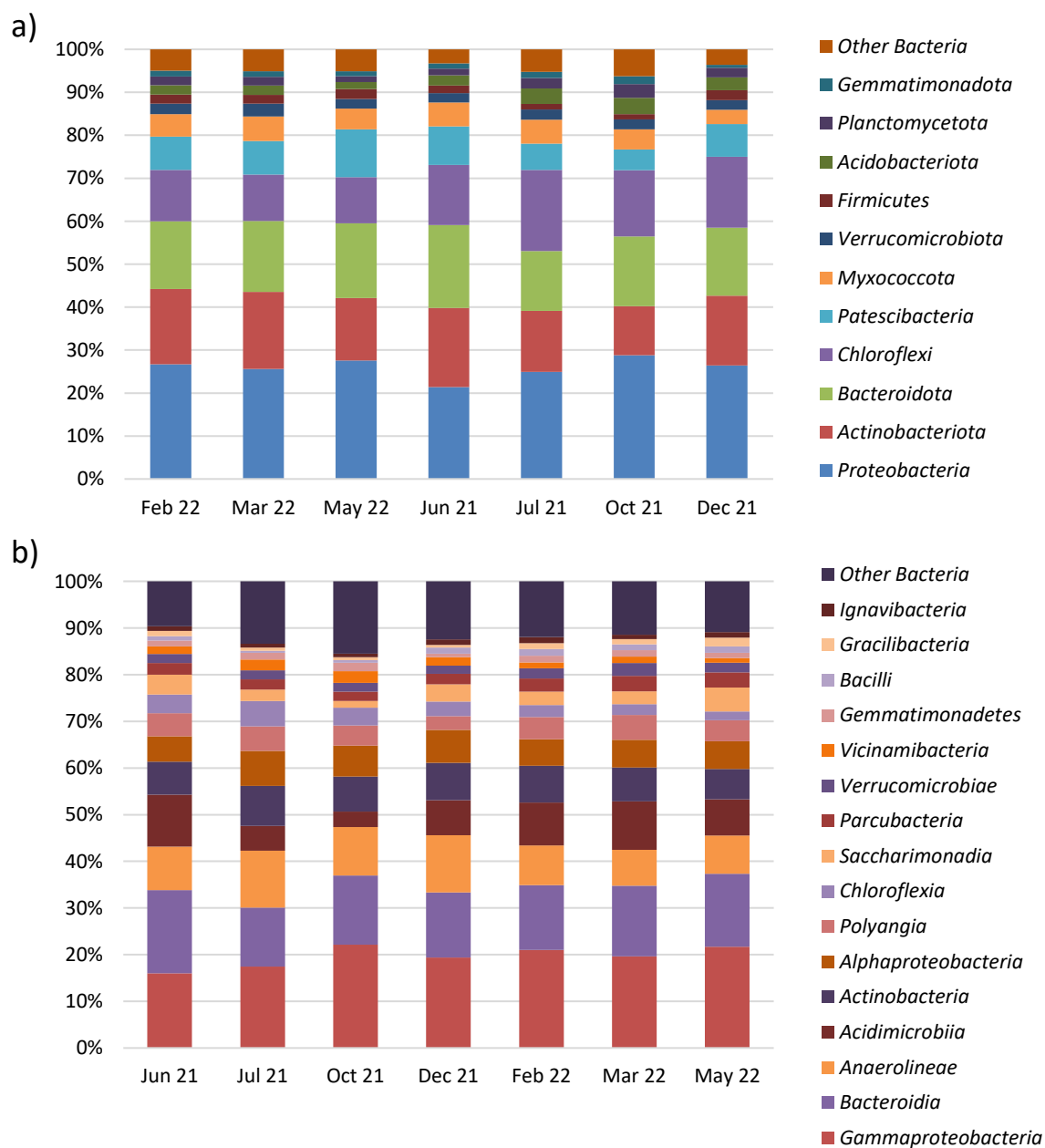


**Figure S4.** Bar chart of the abundance of a) phyla and b) classes in the analyzed samples at each sampling time. Only classes with a mean abundance of more than 1% are shown. The group of other bacteria corresponds to the sum of the unrecognized reads and the classes with low abundance.

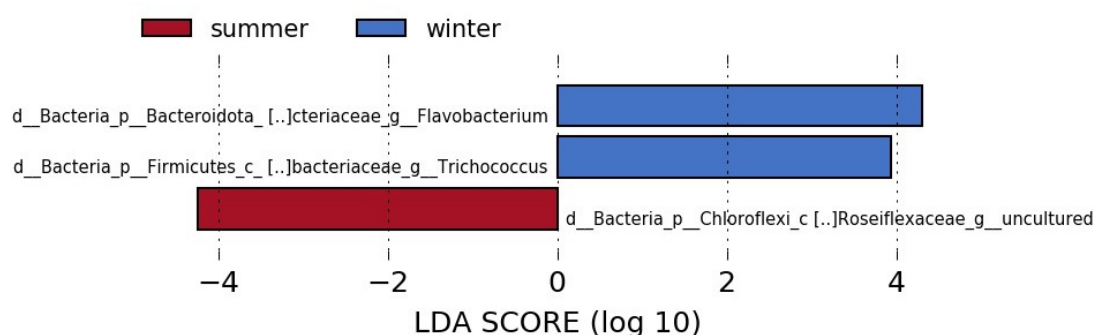


**Figure S5.** Linear discriminant analysis (LDA) effect size (LEfSe) results showing differences in abundance between summer ( $>20^{\circ}\text{C}$ ) and winter ( $<17^{\circ}\text{C}$ ) samples.

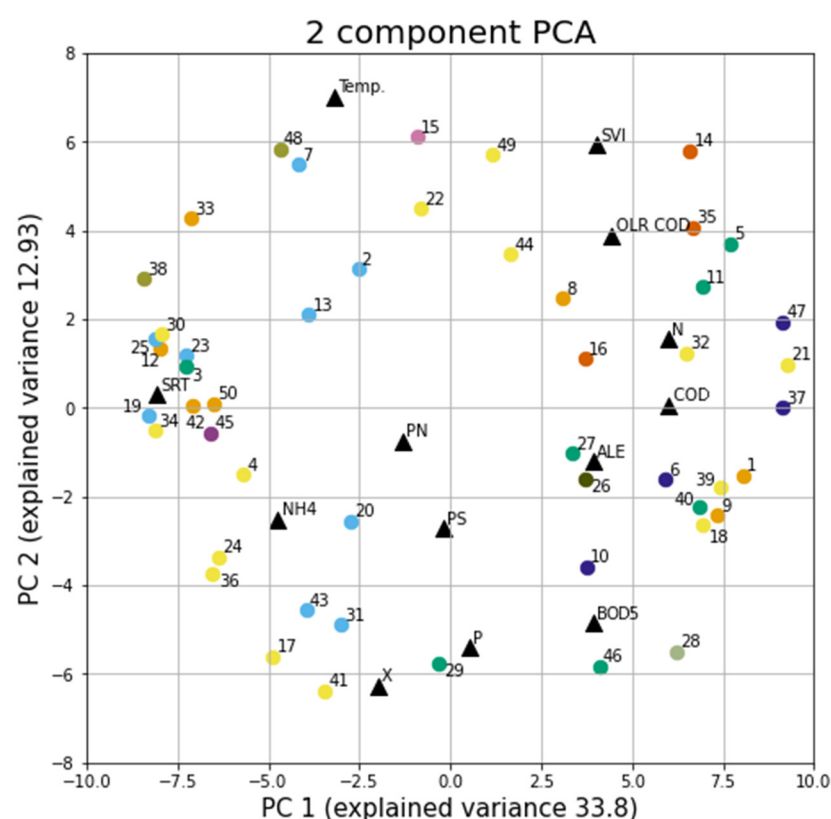


**Figure S6.** Principal component analysis of the fifty most abundant ASVs grouped into ten phyla represented as dots (*Actinobacteriota* (orange), *Chloroflexi* (blue), *Bacteroidota* (green), *Proteobacteria* (yellow), *Patescibacteria* (navy), *Myxococcota* (red), *Gemmatimonadota* (pink), *Nitrospira* (dark gray), *Firmicutes* (light gray), *Acidobacteriota* (khaki), *Planctomycetota* (violet)) and the technological parameters and wastewater quality indices obtained from six time-points (black triangles: Temp.—temperature, SVI—sludge volumetric index, OLR COD—COD loading rate, SRT—sludge retention time, N—total nitrogen in the effluent, COD—COD in the effluent, PN—total PN content in EPS, PS—total PS content in EPS, ALE—content of alginate in activated sludge, NH<sub>4</sub>—ammonium in the effluent, BOD<sub>5</sub>—BOD<sub>5</sub> in the effluent, P—total phosphorus in the effluent, X—concentration of activated sludge in the reactors).

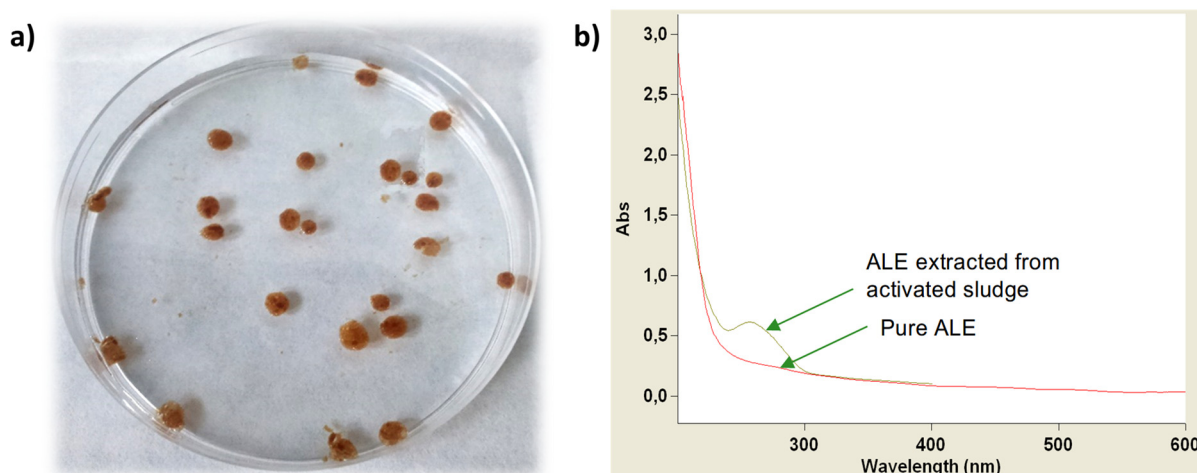


**Figure S7.** Characteristics of recovered ALE: a) gelling properties confirmed by a dropwise addition of ALE solution to  $\text{CaCl}_2$  solution, b) UV-visible spectroscopy results of pure sodium alginate (Sigma-Aldrich) and ALE extracted from waste-activated sludge.

**FT-IR analysis (a detailed description of results is presented in Figures 5 and 6 in the main body of the text)**

The FT-IR/ATR analysis of SOL-, LB-, and TB-EPS revealed that all the spectra contained bands typical of PS, PN, and lipids, the amounts of which vary depending on the season (Fig. 5 in the main body of the text). Fig. 5a presents the FT-IR/ATR spectra of SOL-EPS that were acquired during four seasons (winter, spring, summer, and autumn).

The broad and intensive band at  $\sim 3378\text{ cm}^{-1}$  corresponds to hydroxyl groups in PS as well as N-H in amino groups in primary and secondary amides in PN (amide A) (weakly H-bonded OH and N-H groups) [68]. The band at  $3240\text{ cm}^{-1}$  was caused by vibrations of strongly H-bonded OH- groups and N-H groups in primary and secondary amides. At  $2965\text{--}2857\text{ cm}^{-1}$ , stretching vibrations of aliphatic C-H were observed. The weak bands at  $\sim 1766$ ,  $1731$ , and  $1700\text{ cm}^{-1}$  can be attributed to C=O vibrations of carboxylic acid and esters in lipids and/or pectin. These very low-intensity bands are visible in the spectra of the SOL-EPSs produced in winter and summer. The band at  $1620\text{ cm}^{-1}$  indicates carboxylate ion ( $\text{COO}^-$ ) vibrations and/or C=O in primary amides (amide I band), and the band at  $1546\text{ cm}^{-1}$  corresponds to N-H deformation and C-N stretching (amide II) in PN.

The spectral range between  $1500$  and  $1200\text{ cm}^{-1}$  corresponds to the absorption of lipid head groups, protein amide II (N-H deformation and C-N stretching vibration,  $1500\text{--}1480\text{ cm}^{-1}$ ), amide III (C-N vibrations,  $1400\text{--}1300\text{ cm}^{-1}$ ), and phosphates [66,69]. Nevertheless, the bands at  $1400$  and  $1356\text{ cm}^{-1}$  may also indicate  $-\text{CH}_2$  bending vibrations. Furthermore, the weak bands at  $1467\text{ cm}^{-1}$  and  $1356\text{ cm}^{-1}$  could be caused by vibrations  $-\text{CH}_2$  and  $-\text{CH}$  groups on aliphatic chains, respectively. The peak at  $1419\text{ cm}^{-1}$  can be assigned to the absorption of symmetrical stretching of the carboxyl group [67] or a combination of C-O stretching and OH deformation. Most likely, all these bands overlap. All the spectra have intense absorption bands in the  $1200\text{--}900\text{ cm}^{-1}$  spectral region, due to the high content of carbohydrates (C-O-C and C-OH stretching). The intensity of these bands is lowest in the spectrum of the SOL-EPS sample obtained in autumn.

The bands at  $1170$ ,  $\sim 1082$ , and  $\sim 1055\text{ cm}^{-1}$  point to C-O stretching and C-OH bending vibrations in PS. The band at  $1170\text{ cm}^{-1}$  may also be the result of C-N stretching vibrations or P=O stretching vibrations in phospholipids [66], as well as the bands at  $1055\text{ cm}^{-1}$ . The band at  $990\text{ cm}^{-1}$  can be attributed to phospholipids (P-O-C antisymmetric stretch). The bands with lower wavenumbers ( $900\text{--}700\text{ cm}^{-1}$ ) are characteristic for pyranose and furanose rings as well as  $\alpha$ - and  $\beta$ -glycosidic bonds in PS [67], but they also may be the result of unsaturated C=C bonds [70], N-H deformation vibrations in primary aliphatic amines, N-H wagging vibrations in secondary amines ( $750\text{ cm}^{-1}$ ), and/or C-H out-of-plane

deformation vibration ( $827\text{ cm}^{-1}$ ) [66]. The band at  $614\text{ cm}^{-1}$  is responsible for C=O wagging vibration in esters and/or N-C=O bending vibrations in amides [66]. The spectra analysis indicated that SOL-EPS samples contain PSs, although the analysis of the intensity of the IR bands indicates that the smallest amount of them is found in the samples obtained in spring and autumn. The SOL-EPS samples obtained in summer and winter contain more lipids than the samples obtained in spring and autumn, in which PNs predominate.

The FT-IR spectra of LB-EPS are presented in Fig. 5b. In the spectra of LB-EPS obtained in summer and autumn, vibrations of the C-H groups ( $2963\text{--}2853$ ,  $1377\text{ cm}^{-1}$ ) are visible, which in turn are practically absent in the other two spectra. The same applies to the bands of C=O groups ( $1730$ ,  $925\text{ cm}^{-1}$ ), bands of PN vibrations ( $1562\text{ cm}^{-1}$ ,  $1522\text{ cm}^{-1}$ ,  $1283\text{ cm}^{-1}$  – C-N stretching vibrations), and phospholipids ( $2390$ ,  $1240$ ,  $984$ ,  $925\text{ cm}^{-1}$  – P=O groups vibrations). The bands at  $\sim 1240\text{ cm}^{-1}$  may also indicate sulfate groups [67].

A similar situation occurs in the case of TB-EPS (Fig. 5c), although the bands indicating the presence of PN are much more pronounced and intense than in the case of the SOL- and LB-EPS samples. These bands corresponding to PN have higher intensity in the TB-EPS spectra obtained in summer and autumn, indicating a greater amount of these compounds at those times. Additionally, weak bands at  $\sim 3087\text{ cm}^{-1}$  may indicate the presence of fats with a predominance of unsaturated fatty acids (CH=CH groups vibrations); this band may also be an overtone of the amide II band [66], visible at  $1550\text{ cm}^{-1}$ , which would confirm the high PN content.

The FT-IR/ATR spectra of ALE extracted from activated sludge reveal the presence of PS and PN (Fig. 6 in the main body of the text). As can be seen, the band positions and intensities are similar across seasons, which suggests that there are no significant changes in the chemical composition of ALE during the year. There might be a slight difference in the proportion of guluronic and mannuronic acid residues depending on the season, as suggested by the intensity of the guluronic acid bands ( $968$ ,  $915\text{ cm}^{-1}$ ) and mannuronic acid bands ( $880$ ,  $810\text{ cm}^{-1}$ ) [71]. Additionally, the spectrum of the ALE obtained in autumn is slightly different from the other ALE spectra: the weak band at  $\sim 3087\text{ cm}^{-1}$  (C-H vibration in vinyl =CH<sub>2</sub> group and/or N-H stretching vibration) has the highest intensity, as do the bands at  $\sim 1413\text{ cm}^{-1}$  (C-OH) and  $1723\text{ cm}^{-1}$  (COOH). The proportions between the guluronic and mannuronic acid bands in the autumn ALE spectrum are also different compared to the spectra of ALE obtained in other seasons. Namely, the mannuronic acid bands ( $880$ ,  $810\text{ cm}^{-1}$ ) are slightly more intense than the guluronic acid bands ( $968$ ,  $915\text{ cm}^{-1}$ ). Moreover, the shoulder at  $\sim 1723\text{ cm}^{-1}$ , which is characteristic of C=O symmetric stretching in carboxylic acids and/or esters, is most clearly visible in the autumn spectrum.

Within the  $3600\text{--}3000\text{ cm}^{-1}$  range (broad) stretching vibrations of O-H bonds appeared [72]. Bands around  $3286\text{ cm}^{-1}$  represent the stretching vibration of both the hydroxyl groups of carbohydrates and N-H in amino groups of PN<sup>3,7</sup>. The weak band at  $\sim 3087\text{ cm}^{-1}$  is probably due to C-H vibration in the vinyl =CH<sub>2</sub> group and/or N-H stretching vibration [66]. Stretching vibrations of aliphatic C-H were observed within  $2955\text{--}2853\text{ cm}^{-1}$ .

The bands at  $1646\text{ cm}^{-1}$  and  $\sim 1450\text{ cm}^{-1}$  observed in all spectra correspond to the asymmetric and symmetric stretching of carboxylate COO<sup>-</sup> vibration, respectively [26]. The latter band may also have C-H bending of CH<sub>2</sub> and CH<sub>3</sub> contribution. The band at  $1646\text{ cm}^{-1}$  may also be assigned to amide II vibrations [74,75]. Those bands are very significant and can be used for the characterization of ALE structure [76]. The band at  $1532\text{ cm}^{-1}$  was assigned to the C=C in the pyranose ring [77,78,79] and/or amide I band (N-H bending) in proteins [75]. The band within  $1420\text{--}1400\text{ cm}^{-1}$  was assigned to C-OH deformation vibration with the involvement of the symmetric stretching vibration of O-C-O in the carboxylate group [80]. The peak of very low intensity at  $1330\text{ cm}^{-1}$  was due to the C-N bending vibration in proteins. The band at  $1223\text{ cm}^{-1}$  was assigned to the presence of O-acetyl ester for bacterial ALE [26]. The bands within  $1100\text{--}1010\text{ cm}^{-1}$  can be attributed to the stretching vibration of the pyranosyl ring and the C-O stretching vibrations in carbohydrates<sup>11,15</sup>. The bands below  $1000\text{ cm}^{-1}$  are signature peaks of the two monomers

of ALE, namely, guluronic and mannuronic acids<sup>6</sup>. The band at  $968\text{ cm}^{-1}$  was indicative of C–O stretching vibration in guluronic acid, while the band at  $880\text{ cm}^{-1}$  is indicative of mannuronic acid. The peaks at  $915$  and  $\sim 810\text{ cm}^{-1}$  were assigned to the anomeric C–H deformation vibration of  $\alpha$ -L-guluronic acid and to the C1–H deformation vibration of  $\beta$ -mannuronic acid residues, respectively [26,81]. The weak band at  $782\text{ cm}^{-1}$  is indicative of the ring vibration of pyranose compounds [66].